UDC 681.3.21

AN IMPROVED PREDICTION OF DCT-BASED IMAGE FILTERS EFFICIENCY USING REGRESSION ANALYSIS

Oleksii S. Rubel, Volodymyr V. Lukin

National Aerospace University “KhAI”, Kharkiv, Ukraine

Efficiency of DCT-based filters for a wide-class of images is investigated. The study is carried out for additive white Gaussian noise (AWGN) case with several intensity levels. Local DCT-based filter is used as basic denoising technique. Nonlocal BM3D filter known as the state-of-the-art technique for AWGN removal is also exploited. A precise prediction method of denoising efficiency for several quality metrics is proposed. It is shown that statistics of DCT coefficients provides useful information. Regression models for analyzed filters and metrics are presented. The obtained dependence approximations of quality metrics on DCT statistics have high goodness of fit. One-parameter and multi-parameter fitting cases are considered. The most valuable DCT statistics are found.

Introduction

Noise is the one of the most destructive factors that affects visual quality of images [1]. Loss of visual quality can decrease performance of image processing applications significantly. For instance, quality of images delivered via Internet and networks could be reduced by noise that has appeared at image acquisition stage. Hence, to provide better performance for such applications of noisy images, some image pre-filtering procedure is often needed.

Furthermore, it can be important to assess visual quality of analyzed images. Such knowledge can be helpful for answering the following question: is some filtering needed for image enhancement and can it be beneficial for a given image? If degradation due to present noise is evident in original image and this noise can be eliminated from the image or its region, the answer would be positive. If not, i.e. noise removal leads to loss of image features and visual quality or at least does not result in image enhancement, the answer would be negative. The paper is devoted to answering these questions by analyzing prediction of denoising efficiency using simple statistics.

Quite many efficient image denoising techniques have been proposed in the last decade. Among these techniques, orthogonal transform based filters [2] stand out by their relatively high efficiency. Such filters use some transform to represent signal by its spectrum. Wavelets, discrete cosine (DCT) or other orthogonal transforms are exploited frequently for this purpose. Sparseness and compactness of spectrum representation of a signal allow removing “noisy” spectrum components. High denoising efficiency has been demonstrated by the DCT filter in [3].

Several efficient nonlocal denoising techniques have been proposed recently as well. Nonlocal filters use information redundancy of similar image patches (blocks) collected together and perform collaborative denoising. To our best knowledge, BM3D filter [4] is the state-of-the-art nonlocal technique for AWGN (additive white Gaussian noise) removal. Note that, in addition to similar patch collecting, the BM3D uses DCT as the basis for joint processing of data in patch sets.

It is obvious that image characteristics influence denoising efficiency. In [5], attention was paid to denoising of texture images. For this case, efficiency of the DCT-based filters is low and denoising can sometimes even lead to evident distortions. Meanwhile, such filters can effectively process less complex images. On this basis, it is desirable to have some image characteristics or quantitative parameters in order to carry out rough prediction of denoising efficiency.

Currently, some quality assessments without reference image [6] and efficiency bounds have been proposed [7]. Degradation of locally distributed image features (e.g. decomposition of local image gradient matrix [6]) under noise conditions is one criterion that can be used. Statistics of entire image is used rarely for this purpose. Disadvantage of such an approach is the computational burden which is even higher than filtering itself. Thus, significant requirement arises clearly. Assessment (prediction) of denoising efficiency should have less computational cost than filtering. Certainly, requirement of precise prediction of denoising efficiency should be consistent with computational cost.

The paper is organized as follows. The Section “Brief theory” considers efficient DCT based filter and the proposed prediction method. The next Section “Efficiency prediction method for DCT-based filters” presents some informative graphics to provide better understanding of how the method works. The Section “Preliminaries” describes test database of images and modeling process. Sections “One-parameter fitting” and

"Multi-parameter fitting" show the method performance depending upon the number of DCT statistics used for prediction. "Prediction performance improvement" section presents final method with reduced computational burden.

Brief theory

In our study, two DCT-based denoising techniques were chosen, namely, the DCT filter (its basic version) [3] and the BM3D filter (block matching and 3D filtering) [4]. The general denoising mechanism of these techniques lies in nonlinear block-wise processing of image local spectrum. Its basic task consists in removing "noisy" components. "Noisy" means that the presence of true signal in a certain spectrum component is inessential and noise has the main contribution. It is reasonable to "remove" such spectrum components in blocks and to replace them by zeros (if the so-called hard thresholding is applied)

$$B_{out}(k,l)=\begin{cases} B_{in}(k,l) \leftarrow B_{in}(k,l) > \beta\cdot\sigma, \\ 0 \leftarrow B_{in}(k,l) \le \beta\cdot\sigma, \end{cases} \quad (1)$$

where B_{out} is the filtered spectrum block, β is the adjusting parameter, σ denotes AWGN standard deviation where B_{in} is "noisy" input image spectrum block, and indices for DCT components in each 8x8 block are k = 0..7, l = 0..7. The optimal value of β for wide-class of images lies in the range 2,4…2,8 [8]. Decreasing of denoising efficiency due to non-optimal value setting in this range is insignificant. For simplicity, β value equal to 2,7 and fixed can be used.

It is worth to note that the most efficient denoising is reached in the case of fully-overlapping image blocks. Values in a given pixel that are restored from overlapping blocks containing this pixel are different. To get a joint (final filtered) value, these values are averaged.

The BM3D filter exploits the above mentioned denoising mechanism. This mechanism is applied to a set of blocks collected into 3D array upon condition of their similarity. Therefore, the first procedure called "block matching" finds groups of similar blocks corresponding to a reference one. Such 3D array has essential correlation along the third dimension.

Collaborative denoising is performed on such data array. Along the third dimension, 1D transform is applied. Basically it is Haar transform. In this way, it is easy to eliminate noisy components from highly correlated data. Thus, denoising efficiency on images consisting of groups of similar blocks is usually high. Aggregation of restored blocks into output image is performed in the same way as in the DCT filter.

Note that this denoising mechanism is also restricted especially in the sense of preserving true image details. In other words, there is a certain bound of efficient noise removal without distorting a true signal. Thus, it can be expected that DCT statistics determine denoising efficiency of the analyzed filters. The necessity of such bound assessment is evident.

Statistics of DCT coefficients has been intensively studied. It has been established that probability density function of DCT coefficients is not Gaussian and has heavy tails [9, 10]. Noise presence can significantly change distribution of DCT coefficients compared to noise-free statistics.

In [11], it is shown that denoising efficiency is strictly connected with probabilities $P_{2\sigma}$ and $P_{2,7\sigma}$. Here, $P_{2\sigma}$ denotes value of probability that absolute DCT coefficient value does not exceed 2σ. This parameter shows rough estimation of noise presence in image. In other words, $P_{2\sigma}$ is average amount of noisy components with weak signal constituent which can be missed. $P_{2,7\sigma}$ defines probability that absolute DCT coefficient value exceeds the threshold 2,7σ. This parameter shows amount of kept components or components with strong signal constituent. Note that $P_{2\sigma} + P_{2,7\sigma} < 1$, thus, these probabilities are mutually dependent.

Basically, mean values of $P_{2\sigma}$ and $P_{2,7\sigma}$ are used as characterization parameters of images. Based on them, a prediction technique using linear regression analysis was proposed in [12]. It implies one of two probabilities through the following expressions for predicting the ratio MSE_{out}/σ^2 (where MSE denotes output MSE of DCTF or BM3D filters and AWGN variance σ^2 is assumed a priori known):

$$(MSE_{outDCTF}/\sigma^2)_{est} = -2,63P_{2\sigma}^2 + 2,15P_{2\sigma} + 0,38, \quad (2)$$

$$(MSE_{outDCTF}/\sigma^2)_{est} = 1,86P_{2,7\sigma}^{0,73}, \quad (3)$$

$$(MSE_{outBM3D}/\sigma^2)_{est} = -2,69P_{2\sigma}^2 + 2,2P_{2\sigma} + 0,36, \quad (4)$$

$$(MSE_{outBM3D}/\sigma^2)_{est} = 2,03P_{2,7\sigma}^{0,79}. \quad (5)$$

These expressions have high goodness of fit R^2=0,98 and 0,97 for $P_{2\sigma}$ and R^2=0,94 both for $P_{2,7\sigma}$, where R^2 denotes coefficient of determination [13]. It ranges from 0 to 1 where R^2>0,9 means that most of the variation in the response variable (denoising efficiency) can be explained by modeled variable ($P_{2\sigma}$ or $P_{2,7\sigma}$).

Due to availability of dependences (2)-(5) obtained in advance, one can estimate $P_{2\sigma}$ and $P_{2,7\sigma}$ for a given image before filtering and then to calculate MSE_{out}/σ^2 that characterizes predicted denoising efficiency for the

two considered filters. However, for the presented approximations (3) and (4), a limited number of test images (only eight) and noise levels (only three), was used. As a result, there is a lack of points that correspond to the cases of low efficiency of filters (these are textural images and/or small values of AWGN standard deviation). It means that the cases that are "hard" for the DCT-based filter are considered and taken into account insufficiently.

Afterwards, approximations for other quality metrics were obtained using the same probabilities in [14]. Three metrics were analyzed: MSE/σ^2 as earlier in [12] and two new ones - improvement of PSNR (*IPSNR*) and improvement of PSNR-HVS-M [15] (*IPSNR-HVS-M*), both expressed in dB. The last one is the human vision system based metric that characterizes visual quality of analyzed image with rather high adequateness. The goodness of fit data for the two considered probabilities are presented in Table 1 Expressions for the obtained approximations for MSE/σ^2, *IPSNR* and *IPSNR-HVS-M* for the DCT filter are the following:

$$(MSE/\sigma^2)_{est} = -1{,}45P_{2\sigma}^2 + 0{,}45P_{2\sigma} + 0{,}96, \quad (6)$$

$$(MSE/\sigma^2)_{est} = -1{,}4P_{2{,}7\sigma}^2 + 2{,}25P_{2{,}7\sigma} + 0{,}13, \quad (7)$$

$$IPSNR_{est} = 100 * \exp\left(-\left(\frac{P_{2\sigma} - 1{,}92}{0{,}63}\right)^2\right), \quad (8)$$

$$IPSNR_{est} = 100 * \exp\left(-\left(\frac{P_{2{,}7\sigma} + 0{,}81}{0{,}53}\right)^2\right), \quad (9)$$

$$IPSNR\text{-}HVS\text{-}M_{est} = 100 * \exp\left(-\left(\frac{P_{2\sigma} - 2{,}08}{0{,}67}\right)^2\right), \quad (10)$$

$$IPSNR\text{-}HVS\text{-}M_{est} = 100 * \exp\left(-\left(\frac{P_{2{,}7\sigma} + 0{,}98}{0{,}58}\right)^2\right). \quad (11)$$

Table 1. Goodness of fit (R^2) of the obtained approximations

Metric	$P_{2\sigma}$	$P_{2{,}7\sigma}$
MSE/σ^2	0,978	0,955
IPSNR	0,962	0,935
IPSNR-HVS-M	0,82	0,78

Efficiency prediction method for DCT-based filters

Prediction methods in [12, 14] show high goodness of fitting for metrics MSE/σ^2 and *IPSNR* (see data in Table 1) Meanwhile, the obtained approximations for *IPSNR-HVS-M* are fitted with considerably smaller R^2. This means that it is desirable to provide a better fitting. Note that MSE/σ^2 and *IPSNR* have the same nature (they are strictly interconnected):

$$IPSNR = 10log_{10}(\sigma^2 / MSE). \quad (12)$$

Thus, further we will analyze only the *IPSNR* and *IPSNR-HVS-M* dependencies on $P_{2\sigma}$ and $P_{2{,}7\sigma}$.

Let us consider the estimates of $P_{2\sigma}$ or $P_{2{,}7\sigma}$ obtained for all image blocks. They can be represented as histograms of distributions, two examples of which are presented in Fig. 1. These distributions have been obtained for two test images taken from the database TID2013 [16] (test images №5 and 18) corrupted by AWGN with the same standard deviation (σ = 5). It is seen that shapes of the distributions are slightly different.

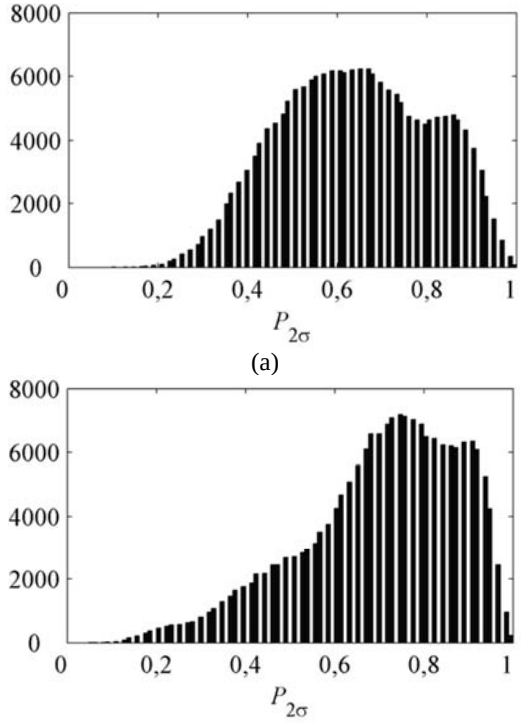

Fig. 1 Examples of $P_{2\sigma}$ distributions

Thus, a distribution of local estimates of $P_{2\sigma}$ or $P_{2{,}7\sigma}$ might contain useful information and such a distribution can be described by one or several statistical parameters. To characterize a distribution, it is possible to employ distribution mean, median, mode, variance, skewness, kurtosis, etc. These parameters are further denoted as *M*, *Med*, *Mod*, *Var*, *S*, and *K*, respectively. Values of these parameters for distribution of local estimates of $P_{2\sigma}$ are given in Table 2 for two analyzed images.

Table 2. Values of statistical parameters for $P_{2\sigma}$

Image	*M*	*Mod*	*Med*	*Var*	*S*	*K*
№5	0,64	0,635	0,635	0,028	2,222	0,06
№18	0,70	0,73	0,73	0,03	3,032	0,708

Clearly, different distributions are characterized by different sets of basic statistical parameters. It is possible to characterize a distribution by different sets of statistical parameters and different number of parameters in a set. So, if we intend to use several statistical parameters for prediction, we should select a proper set and a proper number of parameters which are the most important (informative).

From our previous studies [14], the exponential model (13) seems to be suitable for approximating dependences of the metrics *IPSNR* and *IPSNR-HVS-M* on a considered statistical parameter of the distribution. Besides, such model is simple. This allows assuming that this model can be also exploited for multi-parameter fitting with weighting:

$$Metric_{est} = a^* \exp\left(\sum_{i=1}^{n} b_i O_i(P)\right), \qquad (13)$$

where a and b_i are approximation factors, O_i is some parameter of distribution, n defines the number of such parameters. As O_i, the distribution mean, median, mode, variance, skewness and kurtosis could be chosen. Note that in [12, 14] only the mean of the distribution was used as single statistical parameter. The factors a and b_i, i=1,…,n are to be in advance by multidimensional (n-dimensional) regression.

Such a regression is carried out as follows. There is a set of images corrupted by noise with a set of variance values. These noisy images are filtered with getting *IPSNR* and *IPSNR-HVS-M*. Simultaneously, a considered set of statistical parameters for a given noisy image is estimated. Then, this set of parameters and *IPSNR* (or *IPSNR-HVS-M*) form a multidimensional scatter-plot where statistical parameters serve as function arguments. Having a set of test images and variance values, a set of points is collected. Having such a scatter-plot, an approximation model (13) is fitted and a set of its parameters is obtained.

The choice of statistical parameter(s) is essential for denoising efficiency prediction. Comparison of prediction performance foe different statistical parameters and their combinations will be studied later.

Preliminaries

The first task in n-dimensional regression is to select test images. Images with different content (textures, percentage of pixels that belong to homogenous regions) that have different statistics are needed for our purpose. Values of the considered statistics for the test images must be located over full ranges of possible variation of the considered statistical parameters. Furthermore, for precise approximation of denoising efficiency, a sufficient number of samples (points of the scatterplot) is needed. Some test images are shown below in Fig. 2.

Fig. 2 Some test images

Various types of images could be taken from the database TID2013 [16] (except the test image №25 which is artificial one), all of size 512x384 pixels (see exam-

ples in Fig. 1, a-f). Besides, we have considered several textural test images (e.g., Baboon, Grass, Ground, and Straw, Fig. 1,g-k) were used, all of size 512x512 pixels. In aggregate, we had 34 test grayscale images. Among the test images, there are only real-world images. It is well seen that the used test images have different content.

To meet the requirement of sufficient number of scatterplot points, a number of noise levels should be sufficient, too. The following AWGN levels characterized by noise standard deviation σ are used: 2, 3, 5, 8 10, 15. As a result, there are 204 points that are defined on full axis range both for the metric and statistical parameters.

One-parameter fitting

In this section, the comparison of goodness of fit for different statistical parameters is presented. Goodness of fit R^2 or so-called coefficient of determination (14) is used as criterion of prediction performance. This criterion has been also used in previous studies [12, 14].

There are several definitions of R^2 which are only sometimes equivalent. One class of such cases includes that of simple linear regression. In this case, R^2 is simply the square of the sample Pearson correlation coefficient between the outcomes and their predicted values.

Besides, R^2 is related to mean square error. It describes well performance of prediction using linear regression models. The most general definition of the coefficient of determination is

$$R^2 = 1 - SS_{res} / SS_{tot}, \quad (14)$$

where SS_{res} denotes the sum of squares of residuals, also called the residual sum of squares, SS_{tot} is the total sum of squares which is proportional to the sample variance. Thus, to our opinion, the usage of R^2 will be enough to describe goodness of fit for the considered approximations. Prediction performance for single statistic parameter is shown below in Table 3 for $P_{2\sigma}$ and in Table 4 for $P_{2,7\sigma}$. The best one-parameter approximations are marked by bold.

It is seen that for both probabilities ($P_{2\sigma}$ and $P_{2,7\sigma}$) and for both filters the best approximations for *IPSNR* are those which use mean of distribution. For the *IPSNR-HVS-M* metric, the best approximations are observed for median of distribution. Expressions for prediction of the considered metrics are the following:

$$IPSNR_{est} = a * \exp\left(b_1 \operatorname{mean}(P)\right), \quad (15)$$

$$IPSNR\text{-}HVS\text{-}M_{est} = a * \exp\left(b_1 \operatorname{median}(P)\right). \quad (16)$$

Although median of distributions provides better approximation of *IPSNR-HVS-M*, the obtained results are still not good enough and are worth improving. We expect that this improvement can be gained due to multi-dimensional regression.

Table 3. Goodness of one-parameter fit for $P_{2\sigma}$

	DCT filter		BM3D	
Statistical parameters	*IPSNR*	*IPSNR-HVS-M*	*IPSNR*	*IPSNR-HVS-M*
M	**0,963**	0,767	**0,95**	0,76
Med	0,946	**0,848**	0,932	**0,845**
Mod	0,727	0,813	0,701	0,787
Var	0,085	0,002	0,099	0,008
S	0,145	0,413	0,415	0,395
K	0,428	0,114	0,143	0,11

Table 4. Goodness of one-parameter fit for $P_{2,7\sigma}$

	DCT filter		BM3D	
Statistical parameters	*IPSNR*	*IPSNR-HVS-M*	*IPSNR*	*IPSNR-HVS-M*
M	**0,935**	0,723	**0,921**	0,714
Med	0,919	**0,829**	0,903	**0,823**
Mod	0,619	0,762	0,592	0,721
Var	0,166	0,027	0,187	0,041
S	0,665	0,597	0,643	0,57
K	0,452	0,354	0,44	0,339

In Table 5, the estimated values of approximation factors are presented. The scatter-plots for dependencies of denoising efficiency on one statistical parameters and the fitted curves (approximations shown by solid lines) are represented in Figs 3-4 for single statistical parameters which are the best for a given criterion and filter. Figs 3a-b and 4a-b show *IPSNR* dependencies on statistical parameters, Figs 3c-d and 4c-d present *IPSNR-HVS-M* dependencies.

Table 5. Approximations coefficients values of obtained approximations for $P_{2\sigma}$

Filter	Metric	*a*	b_1
DCT filter	*IPSNR*	0,048	5,606
	IPSNR-HVS-M	0,006	7,271
BM3D	*IPSNR*	0,038	5,899
	IPSNR-HVS-M	0,002	8,41

As it can be seen from Figs 3a-b and 4a-b, the approximations for *IPSNR* metric are well fitted for both filters. Goodness of fit for these cases is expectedly high (see data in Tables 3 and 4). For the *IPSNR-HVS-M* metric, the approximations are fitted not so well; the R^2 values do not exceed 0,85 but the reason is that data are not clustered so well. Such deviation of *IPSNR-HVS-M* values from can be made up by some addition statistical parameter.

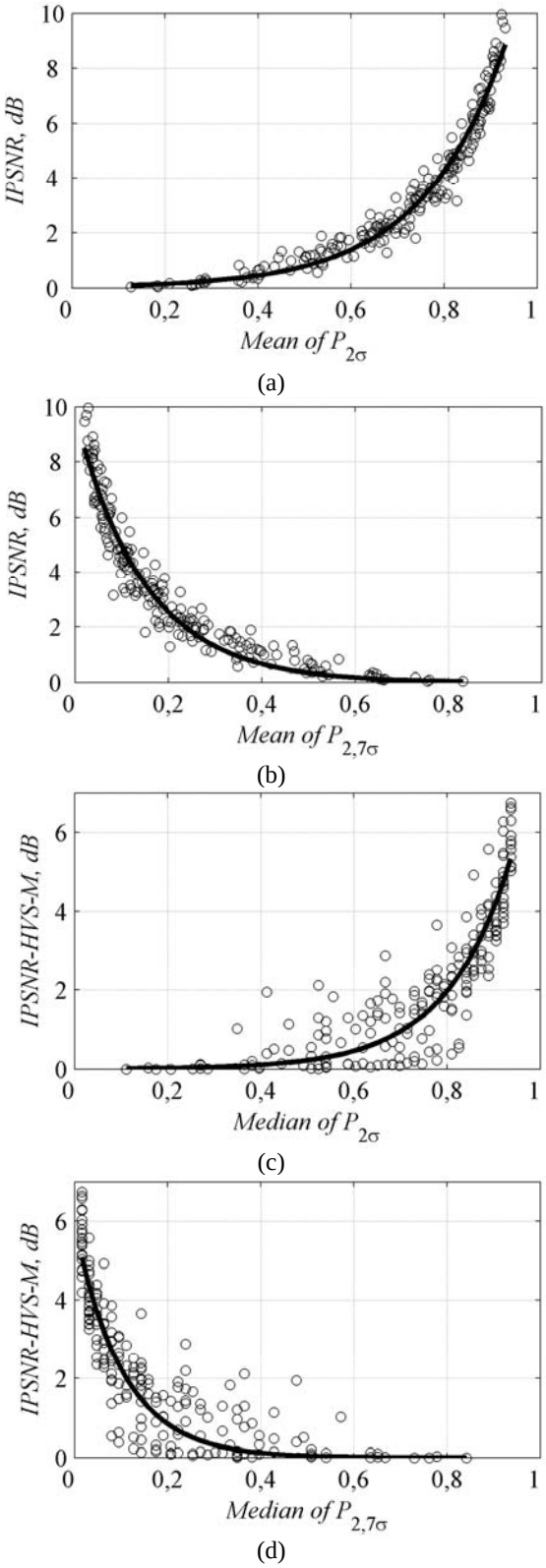

Fig. 3 Scatterplots of DCT filter efficiency on $P_{2\sigma}$ and $P_{2,7\sigma}$ and fitted lines for *IPSNR* and *IPSNR-HVS-M*

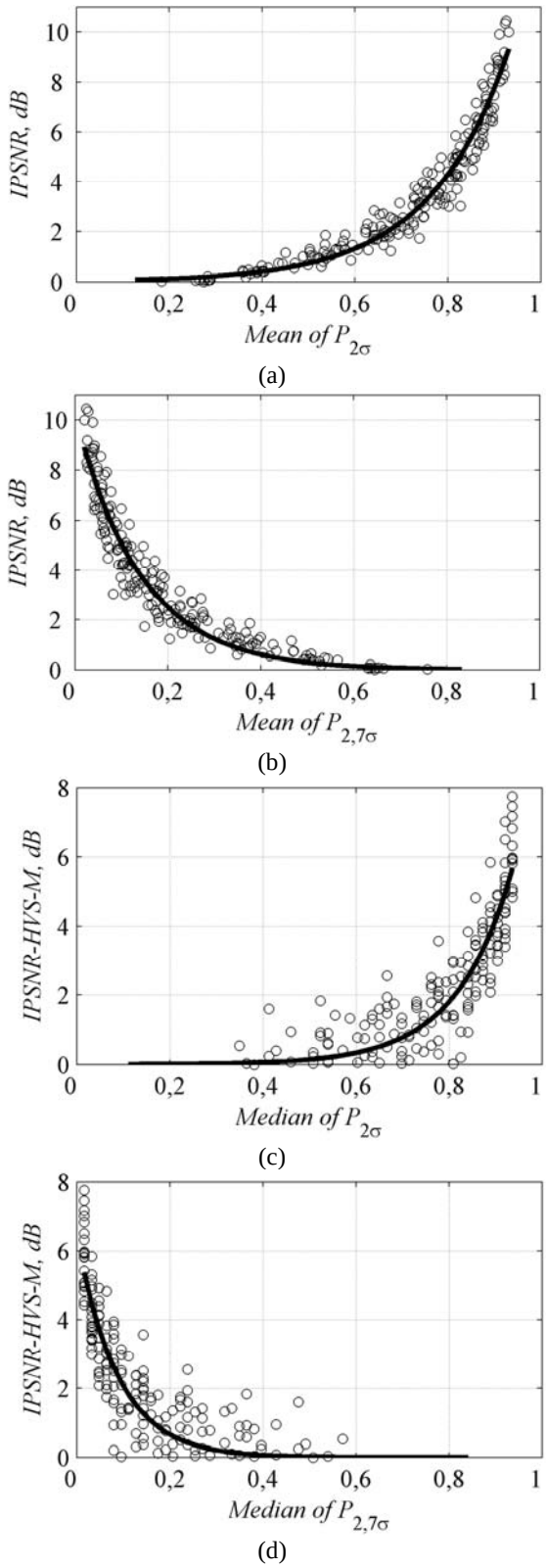

Fig. 4 Scatterplots of BM3D efficiency on $P_{2\sigma}$ and $P_{2,7\sigma}$ and the fitted lines for *IPSNR* and *IPSNR-HVS-M*

In Table 5, the estimated values of approximation factors are presented. The scatter-plots for dependencies of denoising efficiency on one statistical parameter and the fitted curves (approximations shown by solid lines) are represented in Figs 3-4 for single statistical parameters, which are the best for a given criterion and filter. Figs 3a-b and 4a-b show *IPSNR* dependencies on statistical parameters, Figs 3c-d and 4c-d present *IPSNR-HVS-M* dependencies.

Table 5. Approximations coefficients values of obtained approximations for $P_{2\sigma}$

Filter	Metric	*a*	b_1
DCT filter	*IPSNR*	0,048	5,606
	IPSNR-HVS-M	0,006	7,271
BM3D	*IPSNR*	0,038	5,899
	IPSNR-HVS-M	0,002	8,41

As it can be seen from Figs 3a-b and 4a-b, the approximations for *IPSNR* metric are well fitted for both filters. Goodness of fit for these cases is expectedly high (see data in Tables 3 and 4). For the *IPSNR-HVS-M* metric, the approximations are fitted not so well; the R^2 values do not exceed 0,85 but the reason is that data are not clustered so well.

In addition, it should be stressed that statistical parameters of $P_{2\sigma}$ distributions are more suitable than of $P_{2,7\sigma}$ distributions. Onwards, only the statistical parameters of $P_{2\sigma}$ distribution will be used. Both for the sense of behavior and close R^2 values presented approximations are consistent with previously obtained approximations [14]. Note that, in contrast to [14], a simpler approximation model with less number of coefficients is used in this study.

Multi-parameter fitting

It has been shown, that mean or median of $P_{2\sigma}$ are quite good for one-parameter fitting. However, the use of only one parameter can be insufficient for *IPSNR-HVS-M* prediction.

As it has been said, it is possible that the joint use of some combinations of the considered statistical parameters is able to improve prediction. For example, this can be done by including in a set the best statistical parameter obtained for one-parameter fitting and some additional statistical parameters. On one hand, we would like to have less number of statistical parameters used in regression. On the other hand, regression should be improved considerably compared to single parameter case.

To assess mutual connection between analyzed parameters, Spearman rank order correlation coefficient (SROCC) values have been estimated for all possible pairs of statistical parameters (see data in Table 6).

Table 6. SROCC between statistical parameters for $P_{2\sigma}$

	M	*Var*	*Med*	*Mod*	*S*	*K*
M	-	-0,268	0,988	0,906	0,666	0,569
Var	-0,268	-	-0,203	-0,045	-0,078	-0,552
Med	0,988	-0,203	-	0,928	0,697	0,569
Mod	0,906	-0,045	0,928	-	0,625	0,431
S	0,666	-0,078	0,697	0,625	-	0,794
K	0,569	-0,552	0,569	0,431	0,794	-

A high absolute value of SROCC approaching unity means strong connection between statistical parameters. Thus, joint usage of some statistical parameters that are strictly connected is not expected to provide essential improvement. The use of parameters with weak connection can be helpful but not necessarily.

From Table 6, it is seen that mean, median and mode have the highest SROCC and joint use of these parameters would give rather low contribution to prediction. Skewness and kurtosis parameters have intermediate values of SROCC and, probably, can provide some additional information. Variance has lower absolute value of SROCC than other parameters have. Some combinations of variance with other parameters can be suitable.

In Table 7, the best combinations for different numbers of statistical parameters are presented.

Table 7. Goodness of the best multi-parameter fit for $P_{2\sigma}$

Filter	Metric	Statistical parameters	R^2
DCT filter	*IPSNR*	*M*	0,963
		M, Var	0,971
		M, Var, Mod	0,974
		M, Var, Mod, K	0,976
		M, Var, Med, Mod, S	0,977
	IPSNR-HVS-M	*Med*	0,848
		M, Var	0,923
		M, Var, Med	0,926
		M, Var, Med, S	0,927
		M, Var, Med, Mod, S	0,928
BM3D	*IPSNR*	*M*	0,95
		M, Var	0,955
		M, Var, Mod	0,959
		M, Var, Mod, S	0,961
		M, Var, Med, Mod, S	0,961
	IPSNR-HVS-M	*Med*	0,845
		M, Var	0,905
		M, Var, S	0,905
		M, Var, S, K	0,909
		M, Var, Med, S, K	0,917

Note that we have analyzed all combinations of different number of parameters. Note that for the proposed exponential approximation model, the order of parame-

ters is not important. It was found that the combination of all analyzed parameters is inefficient.

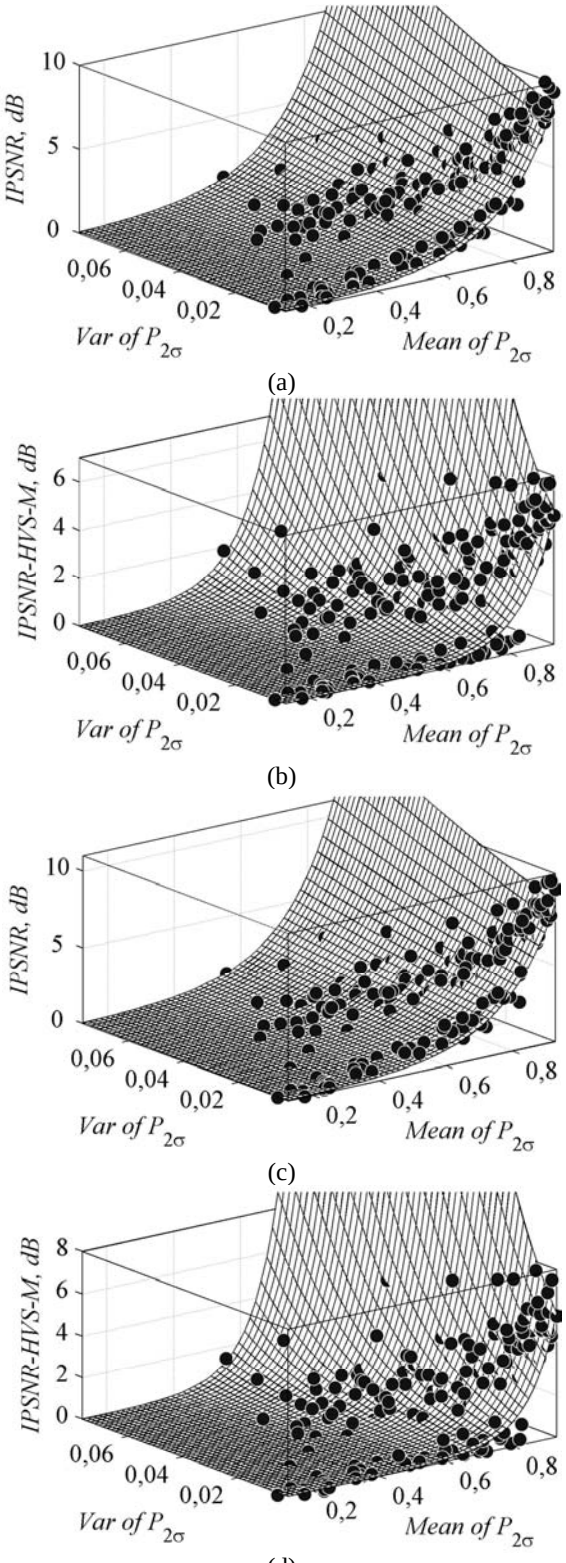

Fig. 5 Scatterplots of DCTF (a, b) and BM3D (c, d) efficiency in $P_{2\sigma}$ and fitted surface for *IPSNR* and *IPSNR-HVS-M*

From the presented data, it is obvious that multi-parameter fitting has larger goodness of fit than one-parameter fitting. Mean and variance of distributions seem to be the most suitable combination of statistical parameters (see the expression (17). These parameters serve as the best combination if two different parameters are used:

$$Metric_{est} = a * \exp\left(b_1 \operatorname{mean}(P_{2\sigma}) + b_2 \operatorname{var}(P_{2\sigma})\right). \quad (17)$$

Adding other parameters does not provide essential improvement of prediction performance. Therefore, the combination of mean and variance of $P_{2\sigma}$ distribution seems to be the most suitable approximation for both metrics and both filters.

Scatter-plots (black circles) of denoising efficiency dependencies on statistical parameters of $P_{2\sigma}$ are shown in Fig 5. The obtained approximations are fitted as surfaces. It can be seen that samples of actual data are scattered over the larger parts of the considered range of arguments. The used parameters are informative and allow predicting the denoising efficiency well enough. The approximation coefficients for all cases are presented in Table 8:

Table 8. Approximations coefficients values of the obtained approximations for $P_{2\sigma}$

Filter	Metric	a	b_1	b_2
DCT filter	*IPSNR*	0,023	6,338	7,459
	IPSNR-HVS-M	$2{,}225*10^{-4}$	10,81	37,14
BM3D	*IPSNR*	0,019	6,591	6,849
	IPSNR-HVS-M	$5{,}324*10^{-5}$	12,42	41,36

Prediction performance improvement

In previous sections, two probabilities, $P_{2\sigma}$ and $P_{2,7\sigma}$, have been used. The threshold options 2σ and $2{,}7\sigma$ have been selected empirically based on values often exploited in the basic DCT denoising mechanism (1). Meanwhile, it has been shown above that $P_{2\sigma}$ is more suitable for prediction than $P_{2,7\sigma}$.

In fact, the proposed method of denoising efficiency prediction assesses amount of noisy components that are small and do not exceed the threshold 2σ. It is mentioned above that noisy DCT components are often weaker than true signal components. In some cases when there is no signal in some DCT component the component value is very small and fully noisy. Thus, some component classification is possible. It is easy to distinguish fully noisy (with signal absence) or weak components, fully-signal (true signal with respectively low noise level) or strong components, and intermediate components. In practice, intermediate components have amplitudes close to the used threshold values, 2σ and $2{,}7\sigma$.

Having the tendency that prediction is better for the threshold 2σ than for 2,7σ, one can expect that a parameter that mainly characterizes percentage of fully-noisy or weak components can work well. This stimulated our interest to selecting parameter β, which is used in threshold setting as βσ for determining the probability that DCT coefficient amplitudes do not exceed this threshold. .

Goodness of fit dependencies on β for the DCT filter and BM3D are presented in Fig. 6. Approximation expression (17) was used in two-parameter fitting. Solid lines for both filters denote dependencies of *IPSNR* approximations; dashed lines depict dependencies of *IPSNR-HVS-M* approximations.

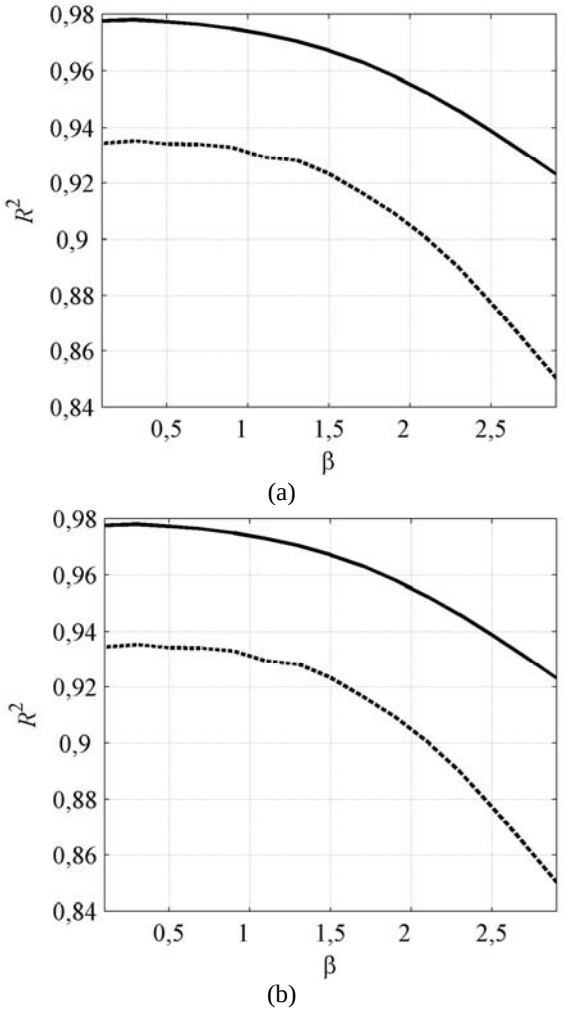

Fig. 6 Goodness of fit depending upon β for the DCT based filter (a) and BM3D (b) in denoising efficiency prediction

It is seen that maximal values of R^2 are observed for β ranging from 0,1 to 0,5. Goodness of fit improvement is essential for β within the range from 0,1 to 0,5 compared to earlier analyzed β=2 or β=2,7.

In Table 9, SROCC between all statistical parameters of $P_{0,1\sigma}$ distribution are given. It is well seen that absolute value of SROCC is high for all pairs of parameters. Prediction performance described by goodness of fit for a set of the most interesting cases is presented in Table 10 for $P_{0,1\sigma}$ distribution.

Table 9. SROCC between statistical parameters for $P_{0,1\sigma}$

	M	*Var*	*Med*	*Mod*	*S*	*K*
M	-	0,891	0,96	0,965	-0,96	-0,911
Var	0,891	-	0,87	0,831	-0,805	-0,887
Med	0,96	0,87	-	0,915	-0,924	-0,892
Mod	0,965	0,831	0,915	-	-0,952	-0,892
S	-0,96	-0,805	-0,924	-0,952	-	0,943
K	-0,911	-0,887	-0,892	-0,892	0,943	-

Table 10. Goodness of the best multi-parameter fit for $P_{0,1\sigma}$

Filter	Metric	Statistical parameters	R^2
DCT filter	*IPSNR*	*M*	0,987
		M, Var	0,989
		M, Var, Mod	0,99
		M, Var, Mod, S	0,991
		M, Var, Med, Mod, S	0,991
	IPSNR-HVS-M	*M*	0,817
		M, Var	0,944
		M, Var, S	0,963
		M, Var, Mod, S	0,963
		M, Var, Med, Mod, S	0,963
BM3D	*IPSNR*	*M*	0,976
		M, Var	0,978
		M, Var, Mod	0,978
		M, Var, Mod, S	0,978
		M, Var, Med, Mod, S	0,978
	IPSNR-HVS-M	*M*	0,812
		M, Var	0,936
		M, Var, S	0,947
		M, Var, Mod, S	0,947
		M, Var, Med, Mod, S	0,948

Goodness of fit for the considered approximations are higher than for previously analyzed case of $P_{2\sigma}$. It should be noted that combinations of statistical parameters are similar to the $P_{2\sigma}$ case. The combination of mean and variance of $P_{0,1\sigma}$ distribution is still the efficient suitable for all cases.

Using the threshold 0,1σ, only the fully-noisy components are exploited for prediction. To add weak signal DCT components into consideration for prediction purpose, it is possible to use the 0,5σ threshold. The use of such a threshold almost does not decrease goodness of fit. SROCC for pairs of statistical parameters of $P_{0,5\sigma}$ is given in Table 11. Goodness of fit data are given in Table 12.

Table 11. SROCC between distribution characteristics for $P_{0,5\sigma}$

	M	*Var*	*Med*	*Mod*	*S*	*K*
M	-	0,207	0,995	0,97	-0,652	-0,212
Var	0,207	-	0,214	0,21	-0,149	-0,782
Med	0,995	0,214	-	0,978	-0,64	-0,213
Mod	0,970	0,21	0,978	-	-0,627	-0,214
S	-0,652	-0,149	-0,64	-0,627	-	0,487
K	-0,212	-0,782	-0,213	-0,214	0,487	-

Table 12. Goodness of the best multi-parameter fit for $P_{0,5\sigma}$

Filter	Metric	Statistical parameters	R^2
DCT filter	*IPSNR*	*M*	0,986
		M, Var	0,989
		M, S, K	0,989
		M, Med, S, K	0,989
		M, Var, Med, Mod, S	0,99
	IPSNR-HVS-M	*Mod*	0,844
		M, Var	0,944
		M, Var, Mod	0,949
		M, Var, Mod, S	0,951
		M, Var, Med, Mod, S	0,952
BM3D	*IPSNR*	*M*	0,975
		M, Var	0,977
		M, Var, S	0,978
		M, Var, Med, S	0,978
		M, Var, Med, Mod, S	0,978
	IPSNR-HVS-M	*Mod*	0,852
		M, Var	0,935
		M, Var, Mod	0,939
		M, Var, Mod, S	0,941
		M, Var, Med, Mod, S	0,941

It is seen that goodness of fit for approximations of $P_{0,5\sigma}$ parameters is almost as high as for the $P_{0,1\sigma}$ case. The differences between R^2 for both probabilities cases are not essential. Note that two-parameter fitting for *IPSNR-HVS-M* case essentially gain goodness of fit is using new specified threshold. For the *IPSNR* case, goodness of fit parameter reaches almost 0,99 that can be interpreted as full metric determination. Also note that R^2 for the DCT filter approximations is higher than for the corresponding BM3D approximations. The approximation (17) coefficients are given in Table 13. Scatterplots of denoising dependencies and the fitted 2D approximations are presented in Fig 7.

Table 13. Approximation factor values of the obtained approximations for $P_{0,5\sigma}$

Filter	Metric	*a*	b_1	b_2
DCT filter	*IPSNR*	0,168	10,8	19,28
	IPSNR-HVS-M	0,01	15,66	144,3
BM3D	*IPSNR*	0,148	11,33	17,7
	IPSNR-HVS-M	0,004	18,25	161,7

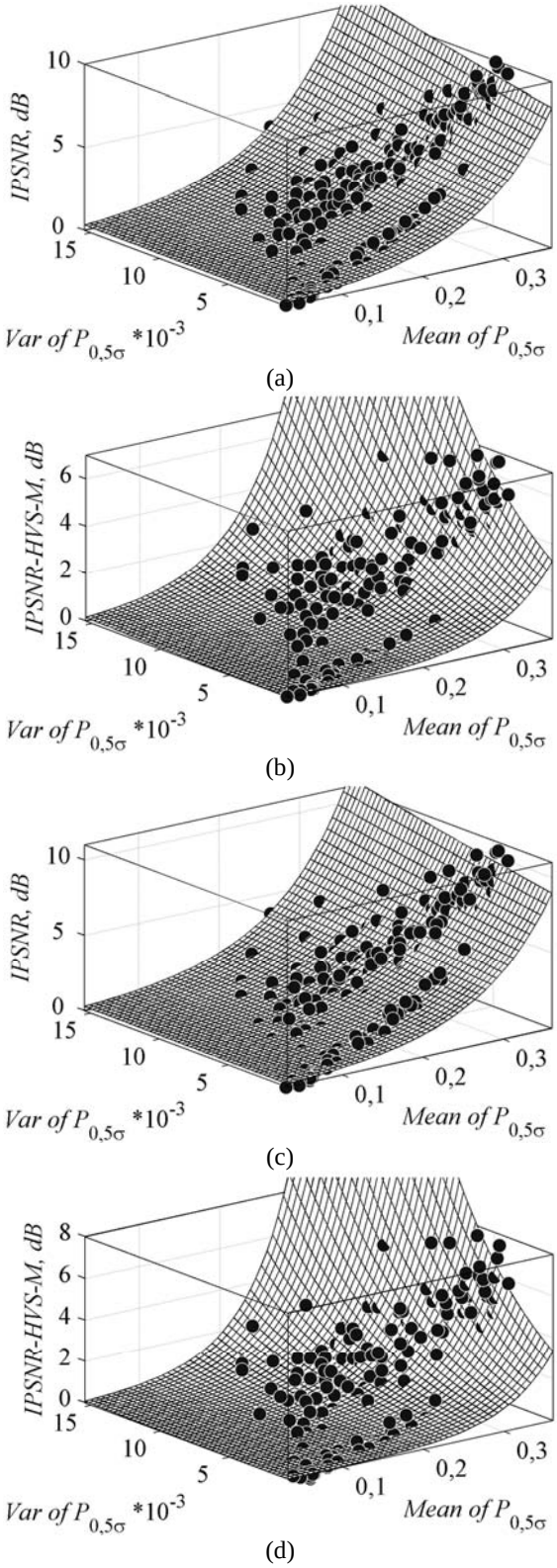

Fig. 7 Scatterplots of the DCT based filter (a, b) and BM3D (c, d) efficiency for statistical parameters of $P_{0,5\sigma}$ and the fitted surfaces for *IPSNR* and *IPSNR-HVS-M*

The final version of the proposed method can be now fully described. The proposed method predicts DCT-based denoising efficiency using either *IPSNR* or *IPSNR-HVS-M* metric or both. Based on such a prediction, it is possible to decide whether to perform some denoising procedure or not. For instance, some observation can be got from obtained scatterplots and fitted approximation surface into it. There is no reason to filter image if the mean of $P_{0,5\sigma}$ does not exceed 0,2. Variance of $P_{0,5\sigma}$ additionally specifies the predicted metric value.

The prediction procedure (original version) includes the following operations. Full-overlapping blocks are used to get DCT statistics. Estimates of used probability in blocks are obtained by simple thresholding operation and one obtains probability distribution (set of local estimates). Afterwards, some statistical parameters of probability distribution are estimated (for example, mean and variance). These parameters are substituted into expression (17) with predetermined factors that we have tabulated. Finally, a predicted metric value is calculated and analyzed.

As we mentioned, the prediction procedure must be as computationally simple. It must be computationally easier than the DCT filter or BM3D. Thus, it is needed to reduce the method complexity without performance degradation. Some ways to do it will be considered.

It is important to determine what computational operations are used and how complex they are. The proposed method uses four operations: 2D DCT in 8x8 blocks, thresholding to estimate probability for each block, statistic data collecting and estimation of statistical parameters of these data, and substitution of these parameters into the obtained approximations. The last one is the simplest. Conversely, first two operations are the most complicated. The third operation complexity depends of number of blocks.

Using full-overlapping blocks in image produces a large number of blocks that must be processed. For each block DCT, which is the most complicated operation in the method, should be done. Thus, it is reasonable to reduce the number of processed blocks. As a result, amount of DCTs and probability estimation operations will be reduced, too. Eventually, estimation of some statistical parameters for local estimate sets (mean and variance of distribution as in (17)) on produced data will be simpler as well.

As it has been mentioned above in the Section “Brief theory”, the considered prediction method assumed data processing in all fully overlapping blocks. Let us consider one possible way to reduce computations. Suppose that it is possible to process less number of non-overlapping or partly overlapping blocks of entire image to get local estimates of the considered probabilities. Such blocks can be chosen arbitrary or according to some rule. A simplest option was chosen in our study. 500 randomly chosen and non-overlapping blocks were used in prediction.

In Fig 8, the scatter-plots of *IPSNR-HVS-M* dependencies on two statistical parameters used in approximation (17) are shown: mean of $P_{0,5\sigma}$ (Fig. 8a) and variance of $P_{0,5\sigma}$ (Fig. 8b). Data of the method that exploits full-overlapping blocks are shown as white circles. In turn, data that are obtained for sparse image sampling using non-overlapping blocks are depicted as black triangles.

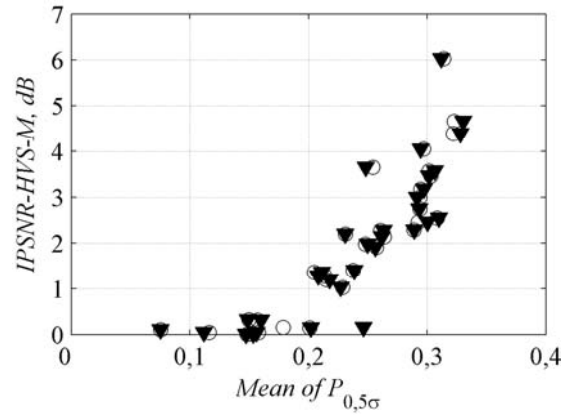

(a)

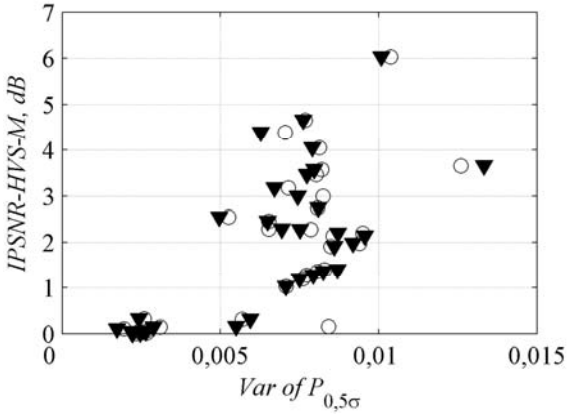

(b)

Fig. 8. Data scatterplots for standard method (that uses full-overlapping blocks) and its sparse version (that exploits 500 randomly chosen non-overlapping blocks)

It is seen that the scatter-plots for both versions of the proposed method are practically the same. Differences between data samples of both cases are small and this means practical possibility of significant decreasing of computations. According to our experiments, 500 randomly chosen non-overlapping blocks are sufficient for efficient prediction of the considered metrics.

Conclusions

The improved method that provides improved prediction of DCT-based image denoising efficiency is proposed. Prediction relates to two types of filters, namely standard DCT based filter with full overlapping of the blocks and hard thresholding and the BM3D filter. Two metrics that describe denoising efficiency - *IPSNR* and *IPSNR-HVS-M* – have been analyzed. It is shown that the first metric can be predicted well enough even if one estimates mean values of one, the most informative local statistic as $P_{2\sigma}$ or $P_{2,7\sigma}$ where the former statistic is better. Moreover, it is shown that other probabilities as $P_{0,5\sigma}$ or $P_{0,1\sigma}$ can serve the goal of prediction even better than $P_{2\sigma}$ or $P_{2,7\sigma}$.

The situation is worse with predicting the metric *IPSNR-HVS-M*. Mean, median or mode of any probability discussed above taken alone does not provide fitting parameter R^2 larger than 0,9. In this case, multi-parameter prediction can be employed.

It has been shown that two-parameter fitting using mean and variance of local probability estimates is the most suitable combination. It produces considerably better fitting than any one-parameter fitting. Multi-parameter fitting is able to provide even better results but the observed improvements are usually negligible.

Although prediction procedure needs less calculation than DCT-based filtering and is much faster than BM3D denoising, prediction can be further accelerated. For this purpose, it is possible to use a limited number of processed blocks (500 or more) which are non-overlapping. Practically no decrease in prediction accuracy is observed.

Future work will be devoted to obtaining prediction approximation for other metrics of image visual quality. More attention will be paid to denoising efficiency prediction for multichannel images and other noise models.

References

1. Pratt, W. K. Digital Image Processing. Fourth Edition / W. K. Pratt. – N. Y.: Wiley-Interscience. – USA. – 2007. – 1429 p.

2. Donoho, D. Nonlinear wavelet methods for recovery of signals, densities, and spectra from indirect and noisy data / D. Donoho // Proceedings Symposium Appl. Math.. – P. 173–205. – 1994.

3. Lukin, V. Image filtering based on discrete cosine transform / V. Lukin, R. Oktem, N. Ponomarenko, K. Egiazarian // Telecommunications and Radio Engineering. – Vol. 66, No. 18. – P. 1685-1701. – 2007.

4. Dabov, K. Image denoising by sparse 3D transform-domain collaborative filtering / K. Dabov, A. Foi, V. Katkovnik, K Egiazarian // IEEE Transactions on Image Processing.- Vol. 16, No. 8. – August 2007. – P. 2080-2095.

5. Image Filtering: Potential efficiency and current problems / V. Lukin, S. Abramov, N. Ponomarenko, K. Egiazarian, J. Astola // Proceedings of ICASSP. – May 2011. – P. 1433-1436.

6. Zhu, X. Automatic parameter selection for denoising algorithms using a no-reference measure of image content / X. Zhu, P. Milanfar // IEEE Transactions on image processing. – Vol. 19, No. 12. – December 2010. – P. 3116-3132.

7. Chatterjee, P. Practical Bounds on Image Denoising: From estimation to information / P. Chatterjee, P. Milanfar // IEEE Transactions on Image Processing. – May 2011. – vol. 20, no. 5. – P. 1221-1233.

8. Fevralev, D. Efficiency analysis of DCT-based filters for color image database / D. Fevralev, V. Lukin, N. Ponomarenko, S. Abramov, K. Egiazarian, J. Astola // Proceedings of SPIE Conference Image Processing: Algorithms and Systems VII, San Francisco, USA. – 2011. – Vol. 7870. – 12 p.

9. Lam, E. A Mathematical analysis of the DCT coefficient distributions for images / E. Y. Lam, J. W. Goodman // IEEE Transactions on Image Processing. – 2000. – vol. 9, no. 10. – P. 1661-1666.

10. Zoran, D. Scale invariance and noise in natural images / D. Zoran, Y. Weiss // IEEE 12th International Conference on Computer Vision. – September 2009. – P. 2209-2216.

11. Pogrebnyak, O. Wiener DCT Based Image Filtering / O. Pogrebnyak, V. Lukin // Journal of Electronic Imaging. – 2012. – No.4. – 14 p.

12. Prediction of Filtering efficiency for DCT-based Image Denoising / S. Abramov, S. Krivenko, A. Roenko, V. Lukin, I. Djurovic, M. Chobanu // 2-nd Mediterrian Conference on Embedded Computing MECO. – June 2013. – P. 97-100.

13. An R-squared measure of goodness of fit for some common nonlinear regression models / C. Cameron, A. Windmeijer, A. G. Frank, H. Gramajo, D. E. Cane, C. Khosla // Journal of Econometrics. – 1997. – vol. 77, no. 2. – 16 p.

14. Rubel, A.S. Prediction of filtering efficiency for discrete cosine transform based removal of additive noise on images / A.S. Rubel, V.V. Lukin // Radio-electronic and computer systems. – 2013. - №4 (63). – P. 35-45. [in Russian].

15. New full-reference quality metrics based on HVS / K. Egiazarian, J. Astola, N. Ponomarenko, V. Lukin, F. Battisti, M. Carli // Proceedings of the Second International Workshop on Video Processing and Quality Metrics, Scottsdale, USA. – 2006. – 4 p.

16. Color Image Database TID2013: Peculiarities and Preliminary Results / N. Ponomarenko, O. Ieremeiev, V. Lukin, K. Egiazarian, L. Jin, J. Astola, B. Vozel, K. Chehdi, M. Carli, F. Battisti, C.-C. Jay Kuo // 4th European Workshop on Visual Information Processing EUVIP2013, Paris, France. – 2013. – 6 p.

Received in final form January 28, 2014